ZIBELINE INTERNATIONAL™ PUBLISHING

Acta Chemica Malaysia (ACMY)

DOI: http://doi.org/10.26480/acmy.01.2022.26.30

ISSN: 2576-6724 (Print)
ISSN: 2576-6732 (Online)
CODEN: ACMCCG

REVIEW ARTICLE

EFFECT OF CHLORO AND NITRO TERMINAL SUBSTITUENTS ON MESOMORPHIC PROPERTIES OF AZOBENZENE LIQUID CRYSTALS

Kamruzzaman, Roushown Ali and Tariqul Hasan*

Department of Chemistry, University of Rajshahi, Rajshahi-6205, Bangladesh
****Corresponding Author E-mail: thasan.chem@ru.ac.bd***

ARTICLE DETAILS

Article History:

Received 02 January 2022
Accepted 10 February 2022
Available online 22 February 2022

ABSTRACT

Substitutent on the mesogen plays a crucial role in determining the shape and mesogenic properties of liquid crystals. In order to evaluate the influence of terminal chloro and nitro substitutions on the structural shape and mesogenic properties, two azobenzene 1-(4-X-phenyl)-2-(4-(hexayloxy) phenyl) diazene (X is Cl or NO_2) liquid crystals have been synthesized by diazotization followed by etherification with hexyl bromide. The structural characterizations of the compound have been performed by spectroscopic methods and studied the mesogenic property by differential scanning calorimetry (DSC) and polarizing optical microscope (POM). Rod-shaped liquid crystals and mesophase formation were obtained by the terminal chloro and nitro substituents of the azobenzene. The textures obtained with polarizing optical microscope (POM) analysis showed enantiotropic smectic A (SmA) mesophase for chloro- and nematic mesophase for nitro substituted azobenzene. Differential scanning calorimetry confirmed two Cr-SmA and SmA-I phase transitions both on heating and cooling.

KEYWORDS

Mesomorphic property, Azobenzene liquid crystals, Terminal substituent, Smectic phase, Nematic phase

1. INTRODUCTION

Since their discovery in 1888, liquid crystals (LC) have become useful in a wide span of applications from biological to optical technology (Carlton et al., 2013; Crwaford et al., 2007; Chapoy, 1985; Stephen and Straley, 1974). Among different shapes of LC molecules, such as rod-, banana- and discotic-shaped, rod-shaped LCs are important for their use both in academic and technological applications (Hudson and Maitlis, 1993). Liquid crystal molecules with rodlike shapes exhibit different orientational and positional order levels in the crystal, smectic, nematic, and isotropic phases to increase the temperature with melting and clearing points (Anna, 2009) (Scheme 1).

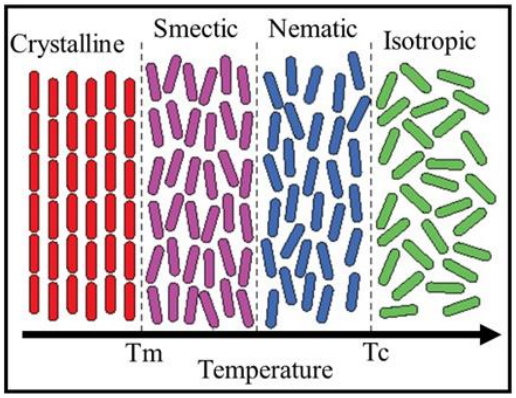

Scheme 1: Different phases of rod-shaped LC

The nematic phase with rodlike molecules is partially aligned in the vertical direction. Nematic liquid crystals usually exhibit a unique state for both liquid and crystalline forms as they show director alignment and can move owing to the deficiency of positional order (Chandrasekhar, 1992; Khoo, 2007). Nematic phases are used as electrically controlled light valves in liquid crystal display (LCD), a typical application of nematic liquid crystals. Like nematics, smectic molecules also show the alignment along the axis of a director and form layers (Scheme 1). Compared to the nematic phase, smectic phases are likely to occur at a lower temperature, maintaining their flexibility because of the weak positional order. Till now, it has been identified about nine different smectic phases with defined features like the amount of positional order within a layer and the direction of the director axis (Collings, 1990; Gray and Goodby, 1984).

The rod-shaped LC molecule consists of a rigid core, a terminal chain, and a lateral substituent (Thompson et al., 2015; Goodby, 2014; Ting et al., 2020). The core provides the rigidity required for anisotropy, whereas the terminal chains provide flexibility to stabilize the molecular alignment within the mesophase. Both nematic and smectic mesophases could be formed depending on the lateral substituent in the rod-shaped LC molecule (Kilic and Cinar, 2007).

Internal changes in rod-shaped LC can also be achieved by changing the polar character in the rodlike molecule (Kapernaum et al., 2012; Romiszewski et al., 2014; Taveres et al., 2010' Rampon et al., 2010; Timmons et al., 2017). In recent decades, azobenzene mesogen-containing rod-shaped LC system has attracted researchers because the reversible photo-isomerization process of azobenzene moieties can profoundly impact the order of mesophase (Zhu and Wang, 2013; Natansohn and Rochon, 2002). The azobenzene-containing molecules form an anisotropic

Quick Response Code	Access this article online	
	Website: www.actachemicamalaysia.com	**DOI:** 10.26480/acmy.01.2022.26.30

Cite the Article: Kamruzzaman, Roushown Ali and Tariqul Hasan (2022). Effect of Chloro and Nitro Terminal Substituents on Mesomorphic Properties of Azobenzene Liquid Crystals. *Acta Chemica Malaysia, 6(1): 26-30.*

phase in trans-conformation, whereas the ordered molecular arrangement is disrupted to form an isotropic phase in cis-conformation. The trans-cis photoisomerization of the azobenzene moiety is promising for various applications, including holographic media, optical storage, reversible optical waveguides, photoalignment of LC systems, and drug delivery (Rochon et al., 1995; Kim et al., 1995; Haus, 2001; Ho et al., 1995; Ichimura, 2000).

Different azo functionalized liquid crystals exhibit a wide variety of mesomorphism and structural phase transitions (Alaasar et al., 2014; Alaasar, 2016; Iamsaard et al., 2016). The terminal substituent of azobenzene-containing molecules plays a vital role in generating mesomorphic behavior and properties for special applications. A wide range of different terminal substituents (e.g., –F, –Cl, –Br, $–NO_2$, $–OCH_3$, OC_2H_5,–CH_3, C_2H_5,) have been incorporated into various liquid crystal molecules (Guan-Yeow et al., 2011; Rabiul et al., 2016; Sourav et al., 2018; Satish and Patil, 1987; Lohar and Jayrang, 1983; Siti et al., 2021; Magdi et al., 2014). The thermal stability and nematic-isotropic phase transition temperature of liquid crystals are greatly affected by terminal substituents' size and polarity nature (Chinnaiyan and Palaninathan, 2015). Terminal substituents having higher polarity will have more thermal attraction resulting in higher nematic-isotropic stability. Thus, the mesomorphic and physical properties of liquid crystal molecules could be controlled by tuning the substituents. Recently, we have reported alkyloxy substituted 4-chloroazobenzene liquid crystals and their mesomorphic properties (Kamruzzaman et al., 2021). In continuation of the previous work, an attempt has been made to synthesize two new calamatics (rodlike) low molecular weight liquid crystal molecules composed of azobenzene as mesogen with terminal substituents (chlorine and nitro groups) and oxyhexyl as a flexible chain. Finally, the mesomorphism properties of azobenzene compounds have been compared based on the terminal chloro- and nitro substituents.

2. Experimental

2.1 Materials

p-Chloro aniline and *p*-nitro aniline were purchased from Loba Chemie Pvt Ltd, India. Sodium nitrite was purchased from Thomas baker (chemicals) limited, India. Hydrochloric acid and phenol were purchased from Merck, Germany, and Merck, India, respectively. K_2CO_3 and 1-Bromo hexane were purchased from Eurostar Scientific Ltd. and Fluka, respectively. All solvents used in this work were purified via distillation followed by refluxed with Na.

2.2 Synthetic procedure of 4-(4-chlorophenyl) diazenyl)phenol (CDP)

The compound CDP was synthesized according to Keller`s methacrylate analog (Santos et al., 2018; Woo-Keun et al., 2006). A 100 mL mixture of PEG400/1,4-dioxane /water (60/30/10) was cooled in an ice bath, and to this mixture, 6.75 mL (78.4 mmol) of concentrated HCl and 5 g (39.2 mmol) of *p*-chloroaniline were added. A solution of $NaNO_2$ (2.98 g, 43.1 mmol) in water (10 mL) was added drop-wise to the above mixture to form the diazonium salt. The solution was left stirring at 0-5 °C for 2 hours. A solution was prepared with phenol (11.07 g, 117.6 mmol) and NaOH (1.72g, 43.1 mmol) in 100 mL of the mixed solvent PEG400/1, 4-dioxane/water (60/30/10) in another flask, and it was poured into the diazonium salt solution. The mixture was stirred for a further 30 min, then water (200 mL) was added. HCl (about 2.5 mL) was added to make the mixture acidic (pH= 5). The solid product (red powder) was filtered off, washed several times with water, and dried in a vacuum. The crude product was purified using petroleum ether/acetone (95/5) as eluent by chromatography as silica gel. The product was obtained as a red powder, yields 5.9 g (65%).

4-(4-chlorophenyl)diazenyl)phenol (CDP): Red powder, yeild: 65%, R_f value 0.43 in petroleum ether: acetone (9:4). ^{1}H NMR ($CDCl_3$, ppm): 6.94 (2H, d), 7.46 (2H, d), 7.83 (2H, d), 7.88 (2H, d), 5.27 (1H, s, Ar-OH) .^{13}C NMR ($CDCl_3$, ppm): 116, 124, 125, 129, 136, 147, 151, 158. IR (KBr, cm^{-1}): 3413, 1638, 1617, 1589, 1576, 1477, 1225, 1082, 838, 724.

2.3 Synthesis of 1-(4-chlorophenyl)-2-(4-(hexayloxy)phenyl) diazene (CDP-H)

The hexyl derivative of **CDP** was synthesized following the procedure [30] as described below:

A mixture of 0.2 g (0.86 mmol) of CDP and 0.48 g (3.45 mmol) of K_2CO_3 was added in 20 mL of dry acetone in a 250 mL round-bottomed flask and stirred for 30 min. Then 1.72 mmol of 1-bromo alkane (1-bromo hexane/1-bromo octane/1-bromo nonane) was added to the mixture, and the reaction mixture was refluxed in an oil bath at 65 °C for 24 hours. The progress of the reaction was monitored by thin-layer chromatography. After completion of the reaction, the mixture was cooled. The residue obtained was filtered off, and the filtrate was concentrated in a vacuum. The solid product obtained was dissolved in 25 mL ether, and this solution was washed with water, 10% sodium hydroxide, and again with water several times. Finally, the ethereal solution was dried over $MgSO_4$. The solution was concentrated in a vacuum, and the crude product was purified by recrystallization in petroleum ether. In each case, the pure product was obtained as orange crystal. The spectroscopic data, i.e., NMR, IR and UV of hexyl derivative of CDP (CDP-H), were as follows.

Orange micro crystal, 0.2 g (75%), R_f value 0.90 in petroleum ether: acetone (9:2). ^{1}H NMR ($CDCl_3$, ppm): 7.88 (2H, d), 7.81 (2H, d), 7.46 (2H. d), 6.98 (2H, d), 4.03 (2H, t), 1.81 (2H, m), 1.48 (2H, m), 1.34 (4H, m), 0.92 (3H, t). ^{13}C ($CDCl_3$, ppm): 14, 23, 26, 29, 32, 68, 115, 124, 125, 129, 136, 147, 151, 162. IR (KBr, cm^{-1}): 2949, 2866, 1637, 1617, 1584, 1501, 1417, 1260, 1138, 1084, 844, 724. UV (nm): 252 ($\sigma \rightarrow \sigma^*$), 356 ($\pi \rightarrow \pi^*$), 448 (n→ π^*).

2.4. Synthetic procedure of 4-(4-nitrophenyl)diazenyl) phenol (NDP)

A 100 mL mixture of PEG400/1,4-dioxane/water (60/30/10) was cooled in an ice bath, and 6.50 mL (74.8 mmol) of concentrated HCl and 5 g (36.2 mmol) of *p*-nitroaniline were added to it. A solution of $NaNO_2$ (2.75 g, 36.8 mmol, in 10 mL water was added drop-wise to the above mixture to form the diazonium salt. The solution was left stirring at 0–5 °C for 2 hours. A solution prepared with phenol (10.23 g, 108.6 mmol) and NaOH (1.74 g, 43.4 mmol) in 90 mL of water was poured into the diazonium salt solution. The mixture was stirred for 30 min and then added 200 mL of water. The mixture was acidified (pH= 5) with HCl (about 2.5 mL). The solid product (red powder) was filtered off, washed several times with water, and dried over P_2O_5 in a vacuum. The crude product was purified by column chromatography on silica gel using petroleum ether/dichloromethane (80/20) as eluent. The product was obtained as a red powder (yields 6.15 g, 70%). The spectroscopic data, i.e., NMR and IR of **NDP** were as follows.

4-(4-nitrophenyl)diazenyl)phenol (NDP): Red powder, yield: 70%, R_f value 0.74 in petroleum ether: acetone (9:5). ^{1}H NMR ($CDCl_3$, ppm): 8.36 (2H, d), 7.98 (2H, d), 7.93 (2H, d), 6.97 (2H, d), 5.26 (1H, s, Ar-OH). IR (KBr, cm^{-1}): 3434, 1633, 1511, 1346, 1139, 854.

2.5 *Synthesis of 1-(4-nitrophenyl)-2-(4-(hexayloxy)phenyl) diazene (NDP-H)*

A mixture of 0.3 g (1.23 mmol) NDP, 0.68 g (4.92 mmol) K_2CO_3 and 20 mL of dry acetone was added in a 250 mL round-bottomed flask and stirred for 30 min. 1-bromo hexane (0.41 g, 2.47 mmol) was then added to the mixture, and it was refluxed in an oil bath at 65°C for 24 hours. All other necessary steps taken were similar to what was carried out for compound CDP-H. The pure product was obtained as orange crystal (yields 0.3 g, 75%). The spectroscopic data, i.e., were as follows.

1-(4-nitrophenyl)-2-(4-(hexyloxy) phenyl)diazene (NDP-H): Orange micro crystal, yield (75%) R_f value 0.58 in petroleum ether : dichloromethane (5:2). ^{1}H NMR ($CDCl_3$, ppm): 8.35 (2H, d), 7.97 (2H, d), 7.95 (2H. d), 7.03 (2H, d), 4.06 (2H, t), 1.83 (2H, m), 1.48 (2H, m), 1.36 (4H, m), 0.92 (3H, t). ^{13}C ($CDCl_3$, ppm): 14, 23, 26, 29, 32, 69, 115, 123, 125, 126, 147, 148, 156, 163. IR (KBr, cm^{-1}): 3467, 2921, 1635, 1523, 1453, 1341, 1294, 1250, 1193, 1113, UV (nm): 252 ($\sigma \rightarrow \sigma^*$), 364 ($\pi \rightarrow \pi^*$), 461 (n→ π^*).

2.6. Analytical Methods

The structure of the compounds was confirmed by spectroscopic analyses. ^{1}H NMR was carried out with BRUKER spectrometer operated at 400 MHz in pulse Flourier Transform mode using chloroform-*d* as solvent. The peak of chloroform-*d* (7.26 ppm) was used as an internal reference. IR spectra were recorded using KBr with PerkinElmer spectrum-100 FT-IR spectrometer. UV-Visible spectra were obtained by using Shimadzu UV-1650PC spectrometer. The enthalpies of transitions (reported in Jg^{-1}) and phase transition temperature were determined by using PerkinElmer DSC-8000. The heating and cooling rate in DSC was 10°C/ min. The textures of the phase transition of the compounds were obtained using Olympus BX53 hot-stage polarizing optical microscope.

3. Results and Discussion

3.1 *Synthesis and structure analysis*

4-(4-chlorophenyl)diazenyl)phenol (CDP) was synthesized by diazotization reaction between *p*-chloroaniline and phenol according to

the procedure described in the experimental section. The synthetic route of the reaction is shown in Scheme 2. The pure CDP was obtained as red powder by chromatographic column separation. The structure of the CDP was confirmed by ^{1}H and ^{13}C NMR analyses.

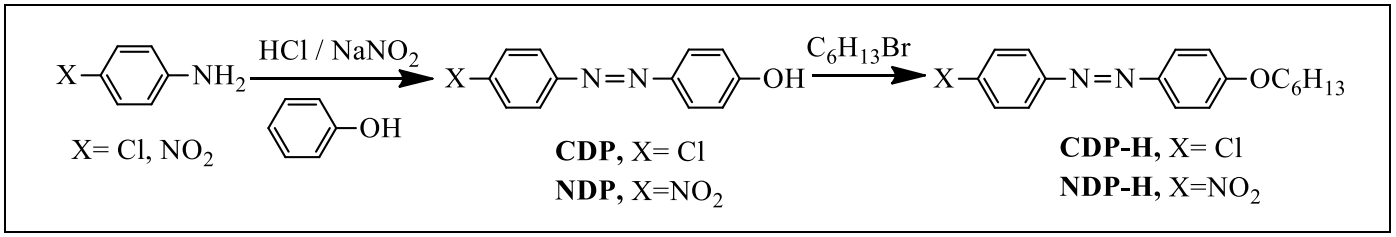

Scheme 2: Synthetic route of 4-(4-chlorophenyl)diazenyl)phenol (**CDP**) and 4-(4-nitrophenyl)diazenyl)phenol **(NDP)**.

In ^{1}H NMR spectrum of CDP (Figure 1A), the signals that appeared in the range of 6.94 –7.88 ppm were assigned for aromatic protons, and a singlet at 5.27 ppm appeared for the Ar-OH proton. In ^{13}C NMR spectrum (Figure 2A) of the compound, four peaks observed in the range of 116 –129 ppm were assigned for the eight carbons of the aromatic ring, and signals appeared at 136, and 147 ppm were assigned for HO-C and Cl-C, respectively. The signals those appeared at 151, and 158 ppm were assigned for two carbons adjacent to the azo group. In the IR spectrum, absorption peaks for –OH and azo groups were appeared at 3413 and 1589 cm^{-1}, respectively. All the spectroscopic data supported the structure of CDP.

The compound CDP-H was synthesized by alkylation of hexyl bromide according to the procedure described in the experimental section. The structure of CDP-H was characterized by spectroscopic analyses. In ^{1}H NMR spectrum (Figure 1B), the signals that appeared in the range of 6.98-7.88 ppm were assigned for aromatic protons, and a triplet at 4.03 ppm was appeared for–OCH_2 protons. The peaks that were observed at 1.81 (2H, m), 1.48 (2H, m), 1.34 (4H, m), and 0.92 ppm (3H, t) were attributed for the aliphatic 11 protons of the hexyl group. In the ^{13}C NMR spectrum of CDP-H (Figure 2B), four peaks appeared in the range of 115–129 ppm were assigned for the eight carbons of the aromatic ring, and peaks for five carbons of the hexyl group were in the range of 14 - 32 ppm. The peak at 68 ppm was assigned for the carbon of –OCH_2 group. The peaks observed at 136 and 147 ppm were assigned for HO-C and Cl-C, respectively. The peaks for two carbons adjacent to the azo group were observed at 151 and 162 ppm. In the IR spectrum, absorption peaks that appeared in the range of 2949-2866 cm^{-1} were identified for C-H stretching vibration, and the signal observed at 1584 cm^{-1} was assigned for the azo group. In the UV spectrum, a $\pi \rightarrow \pi^*$ transition was observed at 357 nm, which indicated the presence of the azo group in the compound.

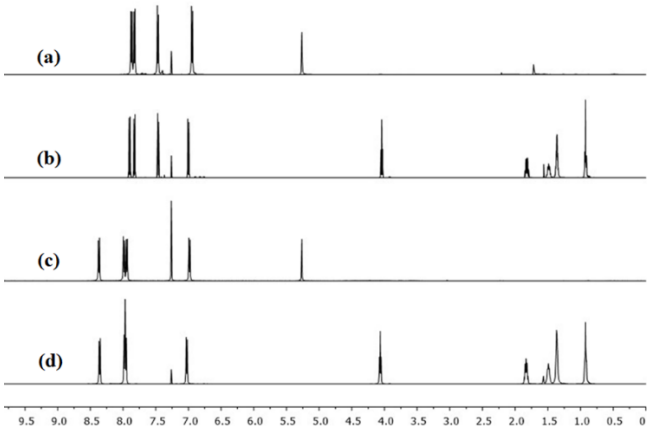

Figure 1: ^{1}H NMR spectra of (a) 4-(4-chlorophenyl)diazenyl)phenol (CDP), (b) 4-(4-nitrophenyl)diazenyl)phenol (NDP), (c) hexyl derivative of CDP (CDP-H) and (d) hexyl derivative of NDP (NDP-H).

4-(4-nitrophenyl)diazenyl)phenol (NDP) was synthesized by diazotization reaction between p-nitroaniline and phenol (Scheme-2)as described in the experimental section. The pure NDP was obtained as red powder by column chromatographic separation. The structure of NDP was confirmed by ^{1}H and ^{13}C NMR analyses.

In the ^{1}H NMR spectrum of NDP (Figure 1C), the signals at 6.97 - 8.36 ppm were assigned for aromatic protons and a singlet at 5.26 for Ar-OH proton. Similar to compound CDP peaks were observed in the ^{13}C NMR spectrum of NDP (Figure 2C) at 116-129, 136, 147, 151, 158 ppm for eight carbons of the aromatic ring, HO-C, Cl-C, and two carbons adjacent to the azo group, respectively. In the IR spectrum, absorption peaks at 3434 and 1633 cm^{-1} were appeared for –OH and azo groups, respectively. The spectroscopic analyses confirmed the structure of NDP.

Similar to the CDP-H, 1-(4-nitrophenyl)-2-(4-(hexyloxy)phenyl)diazene (NDP-H) was synthesized by alkylation of hexyl bromide. Spectroscopic data also supported the structure of NDP-H. Similar spectral peaks have appeared in the ^{1}H and ^{13}C NMR, and UV spectra of NDP-H (Figure 1D), as were observed for the compound CHP-HThe peak for O_2N-C was observed at 148 ppm in ^{13}C NMR spectrum of NDP-H.

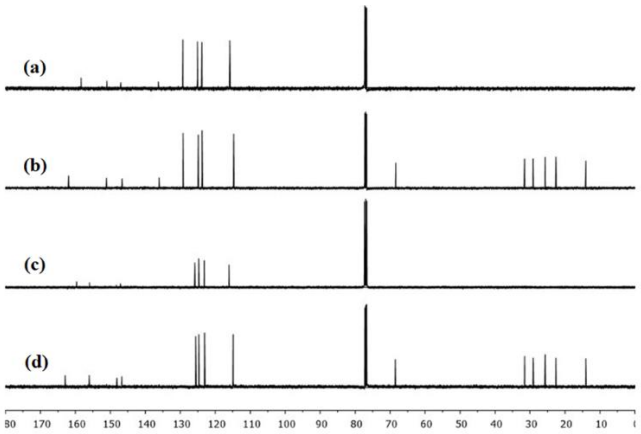

Figure 2: ^{13}C NMR spectra of (a) 4-(4-chlorophenyl) diazenyl)phenol (CDP), (b) 4-(4-nitrophenyl)diazenyl)phenol (NDP), (c) hexyl derivative of CDP (CDP-H) and (d) hexyl derivative of NDP (NDP-H).

3.2 Analysis of mesomorphic behavior

The mesomorphic behavior of the compounds was analyzed by differential scanning calorimetry (DSC) and optical polarizing microscope (POM). The phase transition temperatures associated with transition enthalpies were determined by DSC. 2nd heating and 1st cooling scanning data of CDP-H and NDP-H are summarized in Table 1. The DSC curve of CDP-H is depicted in Figure 3A. Two transitions were observed in both the heating and cooling scan as a result of the enantiotropic phase transition. On the heating scan, the Cr-SmA and SmA-I transitions were observed at 87.66 and 93.26 °C, and on the cooling scan, the I-SmA and SmA-Cr transitions were observed at 89.98 and 62.54 °C.

Similar phase transitions Cr-SmA (at 101°C) and SmA-I (at 168°C), and I-Sm (at 165°C) and SmA-Cr (at 80°C) were observed for N,N′-di-(4′-pentyloxybenzoate)salicylidene-1,3-diaminopropane during heating and cooling, respectively. Rod-shaped azobenzene liquid crystal 1-methoxyalkyloxy-4′-(4-phynylazo)acetophenone also exhibited Cr-SmA-I phase transitions as reported by Salisu et al. (Al-Barody and Ahmad, 2015; Salisu et al., 2009).

Table 1: Phase transition temperatures obtained through DSC scanning on heating and cooling.

Compounds	Transition temperature °C association with transition enthalpy (J/g)	
	2nd Heating	1st Cooling
CDP-H	**Cr** 87.66 (90.21) **SmA** 93.26 (8.51) **I**	**I** 89.98 (15.72) **SmA** 62.54 (83.68) **Cr**
NDP-H	**Cr** 99.07 (125.78) **I**	**I** 96.31 (1.11) **N** 86.87 (117.99) **Cr**

Cr = Crystal, SmA = Smectic A, I = Isotropic, N = Nematic

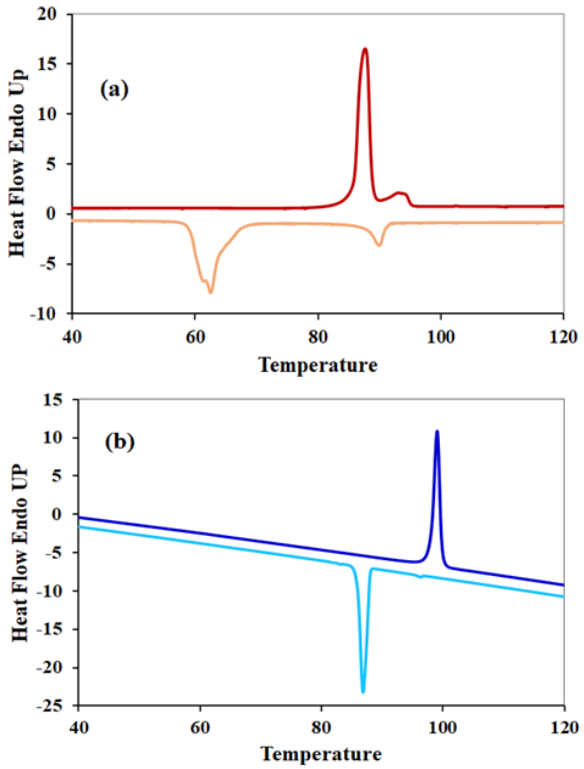

Figure 3: DSC curves obtained on 2nd heating and 1st cooling at 10 °C/min-1, (a) 1-(4-chlorophenyl)-2-(4-(hexyloxy)phenyl)diazene (CDP-H) and (b) 1-(4-nitrophenyl)-2-(4-(hexyloxy)phenyl)diazene (NDP-H).

The DSC curve of the compound NDP-H was depicted in Figure 3B. This compound showed only one phase transition both on heating scan. On the heating scan, the Cr-I transition was observed at 99.07 °C and no liquid crystal was found. On the other hand, the monotropic phase transition was observed on the cooling scan. On cooling scan, the liquid crystal was found at 96.31 °C as nematic mesophase which was disappeared in the crystalization point at 86.87 °C.

The phase textures of CDP-H and NDP-H were studied using a polarizing optical microscope (POM) with a hot stage to identify the mesomorphic phase (Figure 4). The CDP-H was stable during repeated heating and cooling. The DSC and POM data showed a good agreement with each other. For compound CDP-H purely smectogenic, smectic A (SmA) mesophase textures appeared during heating and cooling. This was characterized by battonetes formation on cooling and focal conic fan-shaped structure.

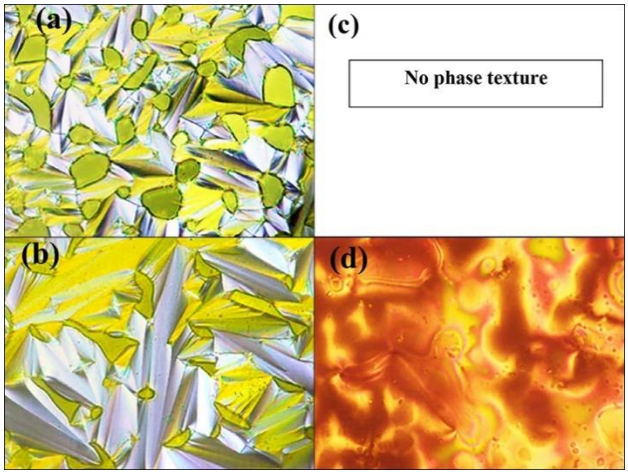

Figure 4: Polarizing optical microscope texture. (a) Smectic A phase to isotropic liquid on heating for CDP-H,(b) Smectic A phase from isotropic liquid on cooling for CDP-H, (c) No phase texture was observed on heating to isotropic liquid for NDP-H and (d) Nematic (N) phase on cooling from isotropic liquid for NDP-H (Cross polarizer magnification × 50).

The Schlieren texture was appeared on the cooling scan, which confirmed the presence of Nematic (N) phase for the compound NDP-H.

3.3 Comparison between CDP-H and NDP-H

CDP-H compound showed enantiotropic liquid crystal with Smectic A (SmA) on both the heating and cooling scan, but NDP-H showed monotropic liquid crystal with Nematic (N) phase on cooling scan. The liquid crystal property shows variation in polarity, polarizability and magnitude of anisotropic intermolecular force of attraction which determines the presence or absence of mesomorphism. In CDP-H, the chloro group is more polarizable and larger in size, which is more favorable for the space-filling concept giving rise to the lamellar packing arrangement, the driving force for forming the smectic phase (Yeap et al., 2009; Imrie and Taylor, 1989). In NDP-H, the bulky nitro group increases the breadth of the terminal benzene ring. The increasing breadth of a molecule increases intermolecular distance and hence decreases intermolecular attraction.

On the other hand, it also increases molecular polarizability, which increases intermolecular attraction. Two opposing effects are operating, while Gray has explained that an increase in the breadth of a molecule decreases both smectic and nematic mesophase stability (Gray, 1958). Therefore, it was assumed that the nitro group not only increases the breadth of the molecule but also increases the acoplanarity in the molecule due to steric interactions. A combination of both breadth and steric effect significantly affects the thermal stability of the ordered arrangement of NDP-H, which results in nematic liquid crystal phase in the only cooling scan.

4. Conclusion

In this work, two low molecular weight azobenzene liquid crystals with chloro and nitro as terminal substituents and hexyloxy flexible units were synthesized. The structures of the compounds were confirmed by spectroscopic analyses. Chloro substituted azobenzene showed enantiotropic Smectic A (SmA) liquid crystal both on heating and cooling scans. On the other hand, nitro substituted azobenzene showed nematic liquid crystal only on cooling scan.

References

Alaasar, M. 2016. Azobenzene-containing bent-core liquid crystals: An overview, Liq. Cryst., 43, pp. 2208–2243. DOI: https://doi.org/10.1080/02678292.2016.1175676

Alaasar, M., Prehm, M., Tschierske, C. 2014. New azobenzene containing bent-core liquid crystals based on disubstituted resorcinol. Liq. Cryst., 41, pp. 126–136. DOI: https://doi.org/10.1080/02678292.2013.840393

Al-Barody S. M. Ahmad, H. 2015. Synthesis, structural characterization and thermal studies of lanthanide complexes with Schiff base ligand N,N′-di-(4′-pentyloxybenzoate)-salicylidene-1,3-diaminopropane, Cogent Chemistry, 1(1), pp. 1093920. DOI: https://doi.org/10.1080/23312009.2015.1093920

Anna, E.F. 2009. A study of optical propagation in polymer liquid crystal nanocomposites for photolithography applications, PhD Thesis, Drexel University. https://www.researchgate.net/publication/28676434

Carlton, R.J., Hunter, J.T., Miller, D.S., Abbasi, R., Mushenheim, P.C., Tan, L.N., Abbott, N.L., D. S. 2013. Chemical and biological sensing using liquid crystals, Liq. Cryst. Rev., 1, pp. 29-51. DOI: https://doi.org/10.1080/21680396.2013.769310

Chandrasekhar, D. 1992. Liquid crystals, 2nd ed. Cambridge, UK: Cambridge University Press.

Chapoy, L.L. 1985. Advances in liquid crystalline polymers, edited by L. L. Chapoy (London: Elsevier). DOI: https://doi.org/10.1007/978-94-009-4934-8

Chinnaiyan, S., Palaninathan, K. 2015. Synthesis, characterization of azobenzene and cinnamate ester based calamitic liquid crystalline compounds and their photoresponsive properties. J. Mol. Struct., 1092, pp. 176-186. DOI: https://doi.org/10.1016/j.molstruc.2015.03.026

Collings, P.J. 1990. Liquid Crystals, Nature's Delicate Phase of Matter. Princeton, NJ, USA: Princeton. University Press.

Crawford, G.P., Woltman, S.J., Jay, G.D. 2007. Liquid crystals: Frontiers in biomedical applications, Singapore: World Scientific.

Goodby, J.W. in Handbook of Liquid Crystals, ed. Goodby, J.W., Collings, P. J., Kato, T., Tschierske, C., Gleeson, H.F., Raynes, P. 2014. Wiley-VCH, Weinheim, 4, pp. 3–41. DOI: https://doi.org/10.1002/9783527671403

Gray, G.W. 1958. Steric effects in conjugated systems; Gray G.W. Ed., Butterworths: London, pp. 160.

Gray, G.W., Goodby, J. 1984. Smectic Liquid Crystals: Textures and Structures, London, UK: Leonard Hill.

Guan-Yeow, Y., Huey-Charn, L., Wan, A.K.M., Corrie, T.I., Daisuke, T., Kohtaro, O. 2011. Synthesis, thermal and optical behaviour of non-symmetric liquid crystal dimers α-(4-benzylidene-substituted-aniline-4′-oxy)-ω-[pentyl-4-(4′-phenyl)benzoateoxy]hexane, Phase Transitions, 84(1), pp. 29-37. DOI: https://doi.org/10.1080/01411594.2010.513613

Haus, H.A. 2001. Linearity of optical amplifiers and the Tomonaga approximation, J. Opt. Soc. Am. B., 18, pp. 1777–1779. DOI: https://doi.org/10.1364/JOSAB.18.001777

Ho, M., Natansohn, A., Barrett, C., Rochon, P. 1995. Azo polymers for reversible optical storage 8. The effect of polarity of the azobenzene groups, Can. J. Chem., 73, pp. 1773–1778. DOI: https://doi.org/10.1139/v95-218

Hudson, S.A., Maitlis, P.M. 1993. Calamitic metallomesogens: metal-containing liquid crystals with rodlike shapes, Chem. Rev., 93, pp. 861-885. DOI: https://doi.org/10.1021/cr00019a002

Iamsaard, S., Anger, E., Aßhoff, S. J., Depauw, A., Fletcher, S.P., Katsonis, N. 2016. Fluorinated azobenzenes for shape-persistent liquid crystal polymer networks, Angew. Chem., 128, pp. 10062–10066. DOI: https://doi.org/10.1002/ange.201603579

Ichimura, K. 2000. Photoalignment of liquid-crystal systems, Chem. Rev., 100, pp. 1847–1873. DOI: https://doi.org/10.1021/cr980079e

Imrie, C.T., Taylor, L. 1989. The preparation and properties of low molar mass liquid crystals possessing lateral alkyl chains, Liq. Cryst., 6(1), pp. 1–10. DOI: https://doi.org/10.1080/02678298908027317

Kamruzzaman, Ali, R., Karim, R., Chowdhury, S. I., Hasan, T. 2021. Effect of flexible chain on mesomorphic properties of alkyloxy substituted 4-chloroazobenzene liquid crystals, Asian J. Chem., 33(5), pp. 1159-1164. DOI: https://doi.org/10.14233/ajchem.2021.23138

Kapernaum, N., Knecht, F., Hartley, C.S. et al. 2012. Formation of smectic phases in binary liquid crystal mixture with huge length ratio", Beilstein J. Org. Chem., 8, pp. 1118-1125. DOI: https://doi.org/10.3762/bjoc.8.124

Khoo, I.C. 2007. Liquid Crystals, 2nd ed. Hoboken, N.J: John Wiley & Sons, Inc.

Kilic, M., Cinar, Z. 2007. Structures and mesomorphic properties of cyano-containing calamitic liquid crystal molecules, J. Mol. Struct. Theochem., 808, pp. 53-61. DOI: https://doi.org/10.1016/j.theochem.2006.12.042

Kim, D.Y., Li, S.K., Tripathy L., Kumar, J. 1995. Laser-induced holographic surface relief gratings on nonlinear optical polymer films, Appl. Phys. Lett., 66, pp. 1166–1168. DOI: https://doi.org/10.1063/1.113845

Lohar, J.M., Jayrang, S.D. 1983. Effect of Nitro Terminal Substituent on the Liquid Crystalline Characteristics of Ester Mesogens: p-Nitrophenyl-p'-n-Alkoxycinnamates, J. Mol. Cryst. Liq. Cryst., 103, pp. 143-153.

Magdi, M.N., Abdelgawad, A.F., Amira, H.A., Gamal, R.S. 2014. Effect of Exchange of Terminal Substituents on the Mesophase Behaviour of some Azo / Ester Compounds, Liq. Cryst., 41(11), pp. 1559-1568.

Natansohn, A., Rochon, P. 2002. Photoinduced Motions in Azo-Containing Polymers, Chem. Rev., 102, pp. 4139–4176. DOI: https://doi.org/10.1021/cr970155y

Rabiul, K., Rezaul, K.S., Rosiyah, Y., Noordini, M.S., Kong, M.L, Ekramul, M. 2016. The effect of terminal substituents on crystal structure, mesophase behaviour and optical property of azo-ester linked materials, Liq. Cryst., 43(12), pp. 1862-1874. DOI: http://dx.doi.org/10.1080/02678292.2016.1216620

Rampon, D.S., Rodembusch, F.S., Gonçalves, P.F.B., et al. 2010. An evaluation of the chalcogen atom effect on the mesomorphic and electronic properties in a new homologous series of chalcogeno esters, J. Braz. Chem. Soc., 21, pp. 2100–2107. DOI: https://doi.org/10.1590/S0103-50532010001100011

Rochon, P., Batalla, E., Natanson, A. 1995. Optically induced surface gratings on azoaromatic polymer films, Appl. Phys. Lett., Vol. 66, Pp. 136–138. DOI: https://doi.org/10.1063/1.113541

Romiszewski, J., Zita Puterova-Tokarova Z, Mieczkowski J, et al. 2014. Optical properties of thiophene-containing liquid crystalline and hybrid liquid crystalline materials. New J. Chem., 38, pp. 2927–2934. DOI: https://doi.org/10.1039/C4NJ00298A

Salisu, A. A., Rahman, M. Z. A., Silong, S., Lutfor, M. R., Ahmad, M. B. 2009. Calamitric azobenzene liquid crystals series: synthesis and mesomorphic properties of 1-methoxyalkyloxy-4-(4-phenylazo)acetophenone", Asian J. Mater. Sci., 1(1), pp. 22-28. DOI: https://doi.org/10.3923/ajmskr.2009.22.28

Santos, A.A.S., Wallison, C.C., Ivan, H.B., Halfen, A.P. R., Aloir, A.M., Leandra, F.C. 2018. Bromine-terminated azobenzene liquid crystals, Liq. Cryst., 46, pp. 655-665. DOI: https://doi.org/10.1080/02678292.2018.1517226

Satish, L., Patil, R.N. 1987. Liquid crystals: effect of substituents on mesomorphic properties, Indian J. Chem., 26A, pp. 815-818.

Siti, N. F. S., Nor, M.M.A.R, Rabiul, K., Idayu, Z., Noordidi, M.S. 2021. Effects of lateral methyl and terminal substituents on thermal, mesomorphic and optical properties of azo-ester mesogens, J. Mol. Struct., 1225, pp. 129112. DOI: https://doi.org/10.1016/j.molstruc.2020.129112

Sourav, P., Golam, M., Nazma, B., Atiqur, R.L., Santanu, K.P., Nandiraju, V.S.R, Aloka, S. 2018. Cybotactic nematic phase of achiral unsymmetrical bent-core liquid crystals – Quelling of polar ordering and the influence of terminal substituent moiety, J. Mol. Liq., 257, pp. 144-154. DOI: https://doi.org/10.1016/j.molliq.2018.02.097

Stephen, M.J., Straley, J.P. 1974. Reviews of Modern Physics, 46(4), pp. 617-704. DOI: https://doi.org/10.1103/RevModPhys.46.617

Tavares, A., Ritter, O.M.S., Vasconcelos, U.B., et al. 2010. Synthesis of liquid-crystalline 3, 5-diarylisoxazolines, Liq. Cryst., 37, pp. 159–169. DOI: https://doi.org/10.1080/02678290903432098

Thompson, M., Carkner, C., Mosey, N.J., Kapernaum, N., Lemieux, R.P., 2015 Tuning the mesomorphic properties of phenoxy-terminated smectic liquid crystals: the effect of fluoro substitution, Soft Matter, 11, pp. 3860-3868. DOI: https://doi.org/10.1039/C5SM00473J

Timmons, D.J., Jordan, A.J., Kirchon, A.A., et al. 2017. Asymmetric flavone-based liquid crystals: synthesis and properties, Liq. Cryst., 44, pp. 1436–1449. DOI: https://doi.org/10.1080/02678292.2017.1281450

Ting, T.X., Sarjadi, M.S., Rahman, M. L. 2020. Influences of central units and terminal chains on the banana-shaped liquid crystals, Crystals, 857, pp. 1-42. DOI: https://doi.org/10.3390/cryst10100857

Woo-Keun, L., Kyu-Nam, K., Marie, F.A., Jung-Il, J. 2006. Dimesogenic compounds consisting of cholesterol and fluorinated azobenzene moieties: dependence of liquid crystal properties on spacer length and fluorination of the terminal tail, J. Mater. Chem., 16, pp. 2289-2297. DOI: https://doi.org/10.1039/B516141J

Yeap, G.Y., Hng, T.C., Yeap, S.Y., et al. 2009. Why do nonsymmetric dimers intercalate? The synthesis and characterisation of the α(4benzylidenesubstituted aniline4'oxy)ω(2methylbutyl4' (4''phenyl)benzoateoxy)alkanes", Liq. Cryst., 36, pp. 1431–1441. DOI: https://doi.org/10.1080/02678290903271504

Zhu, Y., Wang, X. 2013. Synthesis and photoresponsive properties of two liquid crystalline polymers bearing branched azobenzene-containing side chains, Polym. Chem., 4, pp. 5108–5118. DOI: https://doi.org/10.1039/c3py00757j